Rapid Diagnosis Method for Transplutonium Isotopes Production in High Flux Reactor

Qingquan PAN[1*], Qingfei ZHAO[1], Lianjie WANG[2], Bangyang XIA[2], Yun CAI[2], Xiaojing LIU[1*]

panqingquan@sjtu.edu.cn, xiaojingliu@sjtu.edu.cn

1. School of Nuclear Science and Engineering
Shanghai Jiao Tong University
Shanghai, 200240, China

2. Science and Technology on Reactor System Design Technology Laboratory
Nuclear Power Institute of China
Chengdu, 610200, China

Corresponding Author: Qingquan PAN
School of Nuclear Science and Engineering
Shanghai Jiao Tong University
Shanghai, 200240, P. R. China
Email: panqingquan@sjtu.edu.cn
Tel: +0086-13751110835

Corresponding Author: Xiaojing LIU
School of Nuclear Science and Engineering
Shanghai Jiao Tong University
Shanghai, 200240, P. R. China
Email: xiaojingliu@sjtu.edu.cn
Tel: +0086-13761043485

ABSTRACT

Transplutonium isotopes are scarce and need to be produced by irradiation in high flux reactors, but their production is inefficient and optimization studies are needed. This paper analyzes the physics nature of transplutonium isotopes production

by taking Cf-252, Cm-244, Cm-242 and Pu-238 as examples. Traditional methods based on the Monte Carlo burnup calculation are faced with the shortcomings of large amounts of calculation and are unable to analyze the individual energy intervals in more detail, thus cannot support the refined evaluation, screening and optimization of the irradiation schemes. After grasping the physics nature and simplifying the complexity of the production process, we proposed a rapid diagnosis method for evaluating the radiation schemes based on the concept of "Single Energy Interval Value (SEIV)" and "Energy Spectrum Total Value (ESTV)". The rapid diagnosis method can not only avoid the tedious burnup calculation but also help to provide direction for optimization. The optimal irradiation schemes for producing Cf-252, Cm-244, Cm-242 and Pu-238 are determined based on the rapid diagnosis method. The optimal irradiation schemes can greatly improve production efficiency. Compared with the initial scheme, the optimal scheme improves the production efficiency of Pu-238 by 7.41 times, 11.98 times for Cm-242, 65.20 times for Cm-244 and 15.08 times for Cf-252, respectively. The work in this paper realizes the refined analysis of transplutonium isotopes production and provides a theoretical basis for improving production efficiency.

***Keywords*:** Transplutonium isotopes, Rapid Diagnosis Method, Production optimization, Single Energy Interval Value, Energy Spectrum Total Value.

1. INTRODUCTION

Transplutonium isotopes [1] refer to nuclides with an atomic number greater than or equal to 94 (plutonium element). Most are radioactive isotopes with unstable nuclei and can spontaneously release rays (α, β, γ) or neutrons by spontaneous fission. Transplutonium isotopes mainly include: the 94th element plutonium (Pu), the 95th

element americium (Am), the 96th element 96 curium (Cm), the 97th element berkelium (Bk), the 98th element californium (Cf), et al. All transplutonium isotopes are metals, as shown in Figure 1. Because of their research and application value, transplutonium isotopes have attracted extensive scientific attention [2-4].

Figure 1. The photographs of plutonium, americium and berkelium, californium

Transplutonium isotopes are more scarce and expensive than medical isotopes [5-8]. For example, Cf-252 is the most expensive element, at $27m a gram, 650,000 times more than gold. Cf-252 is a strong neutron source, emitting 2.35×10^6 neutrons per microgram per second with a half-life of 2.65 years. Cf-252 releases neutrons in a spectrum similar to a fission reactor, making it an ideal source of neutrons for reactor start-up [9]. Cf-252 is also effective in the treatment of cervical cancer [10], in oil exploration [11], and in prompt gamma neutron activation analysis (PGNAA) [12], et al. Pu-238 is widely used in the radioisotope thermoelectric generator because of its moderate half-life, high thermal power density and easy radiation protection from α decay [13]. Cm-242 and Cm-244 are portable α-ray sources that can power satellites and spacecraft, and they are also used as target materials to produce Cf-252 [14].

Most transplutonium isotopes do not exist naturally and must be produced [15-18]. There are three methods of production: 1) production in accelerators [19], 2) production during a thermonuclear explosion [20], and 3) production during irradiation in a high flux reactor [21]. Among them, irradiation in a high flux reactor is the most stable and efficient production method, and it is the only way to produce Cf-252 in commercial operation. Only two laboratories worldwide can stably produce Cf-252 using a high-flux irradiated curium target [22]. One is the Oak Ridge National Laboratory (ORNL) in the United States, and the other is the Research Institute of

Atomic Reactors (RIAR) in Russia. However, worldwide production of transplutonium isotopes remains low. In 78 production runs over the past 60 years [23], only 1.2 grams of Bk-249, 10.2 grams of Cf-252, 39 milligrams of Es-253, and 15 picograms of Fm-257 were produced through the High Flux Isotope Reactor (HFIR) [24] and the Radiochemical Engineering Development Center (REDC) [25] in the United States.

Neutron capture reactions and decay reactions occur during the production by reactor irradiation [26-27]. For each neutron absorbed by a nuclide, the atomic number of the nuclide increases by one, becoming a new nuclide. So the target material changes from nuclides with a small mass number to nuclides with a large mass number through a series of nuclear reactions (radiation capture, β-decay). Figure 2 shows the nuclide conversion process of producing transplutonium isotopes in a high flux reactor [28].

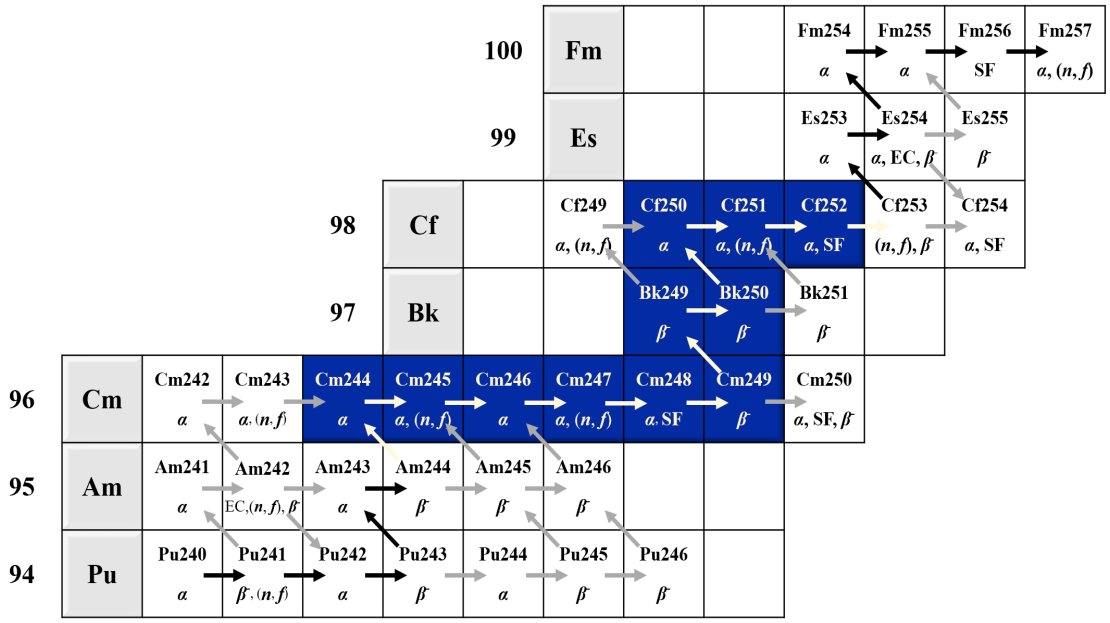

Figure 2. Nuclide conversion process of producing transplutonium isotopes

Besides the absorption reaction, the fission reaction also occurs. Once the fission reaction occurs, the production of transplutonium isotopes is stopped, causing the fission losses and leading to a low conversion rate. Therefore, the fission reaction

should be reduced while the absorption reaction should be increased to improve production efficiency. Because the cross section is related to the neutron spectrum [29-30], the neutron spectrum around the target should be studied. The neutron spectrum around the target greatly influences production efficiency [31]. To summarize the literature review, two questions should be answered to improve the production efficiency of transplutonium isotopes: 1) how to find the optimal neutron spectrum, and 2) how to achieve the optimal neutron spectrum. The background of optimization of transplutonium isotopes production is shown in Figure 3.

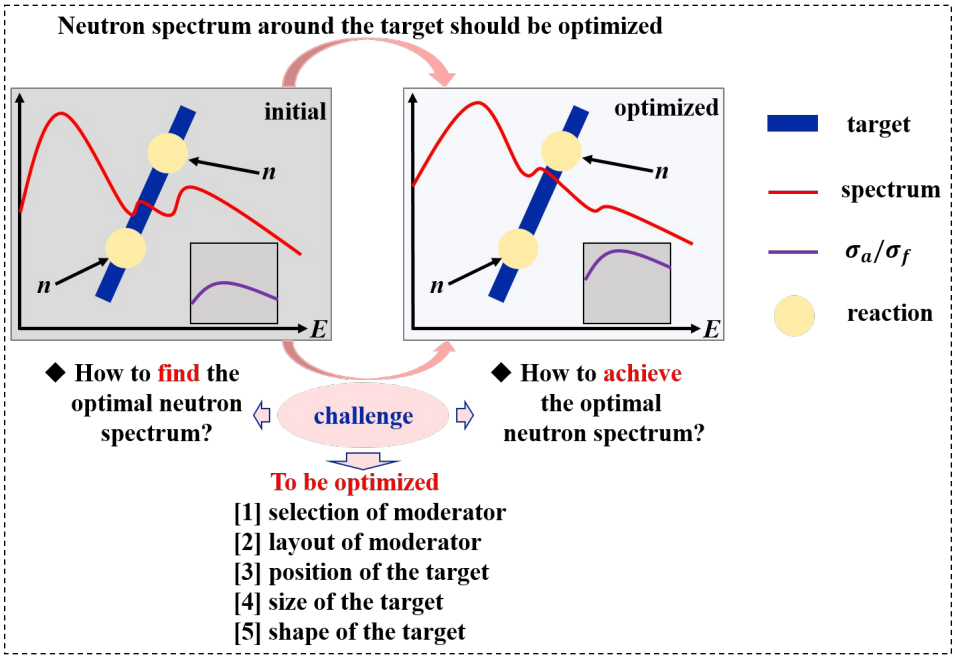

Figure 3. The background of transplutonium isotopes production optimization

For answering the first question, it is difficult to find the optimal neutron spectrum because of the high complexity of the production process, and there is still no corresponding Neutronics model that can analyze each energy interval individually. Traditional methods search for the optimal neutron spectrum by a large number of Monte Carlo burnup calculations. The burnup equation is independent of energy, so it is impossible to perform multi-group burnup calculation. Therefore, the traditional methods take many computations, and can only macroscopically analyze the whole energy spectrum, not the particular energy intervals in more detail, thus cannot support the refined evaluation, screening and optimization of the irradiation

scheme. So we need a rapid diagnosis method for transplutonium production. Grasping the essence of the production process and simplifying the complexity to achieve the refine Neutronics analysis, so as to support the optimization, improve the production efficiency and reduce the production cost.

For answering the second question, the neutron spectrum has a complex relationship with the design parameters, so it is necessary to perform reactor physics calculations [32-34] and sensitivity analysis. After the sensitivity analysis of some design parameters to production efficiency, we can achieve the optimal neutron spectrum by optimizing these design parameters, such as 1) the selection of the moderator, 2) the layout of the moderator, 3) the position of the target, 4) the size of the target, and 5) the shape of the target. We try to adjust these parameters to obtain a production scheme with high efficiency, that is, by adjusting these parameters to obtain an optimal neutron spectrum for producing transplutonium isotopes.

This paper analyzes the optimization method of transplutonium isotopes production by taking Cf-252, Cm-244, Cm-242 and Pu-238 as examples. By proposing the concepts of “Single Energy Interval Value (SEIV)” and “Energy Spectrum Total Value (ESTV)”, we establish a rapid diagnosis method and realize the detailed analysis of the energy spectrum around the target. The rapid diagnosis method can not only avoid the tedious burnup calculation but also help to provide direction for optimizing the irradiation scheme. Then, an optimal irradiation scheme is proposed after the sensitivity analysis based on the rapid diagnosis method. The paper is organized as follows: Chapter 2 introduces the rapid diagnosis method, Chapter 3 gives numerical and experimental verification, Chapter 4 introduces the optimal process based on sensitivity analysis, and Chapter 5 gives a conclusion.

2. RAPID DIAGNOSIS METHOD

2.1 The High Flux Reactor

All analyses are performed in a high flux lead-bismuth reactor that is under

design. It has a 90-day refueling cycle with the highest flux of 6.7×10^{15}. The inlet temperature is 170℃, the outlet temperature is 536.5℃, and the coolant velocity is 4.0 m/s. ^{208}Pb-Bi is used as the coolant, and ^{208}Pb is used as the reflector layer. Figure 4 shows the X-Y and X-Z sections of the reactor.

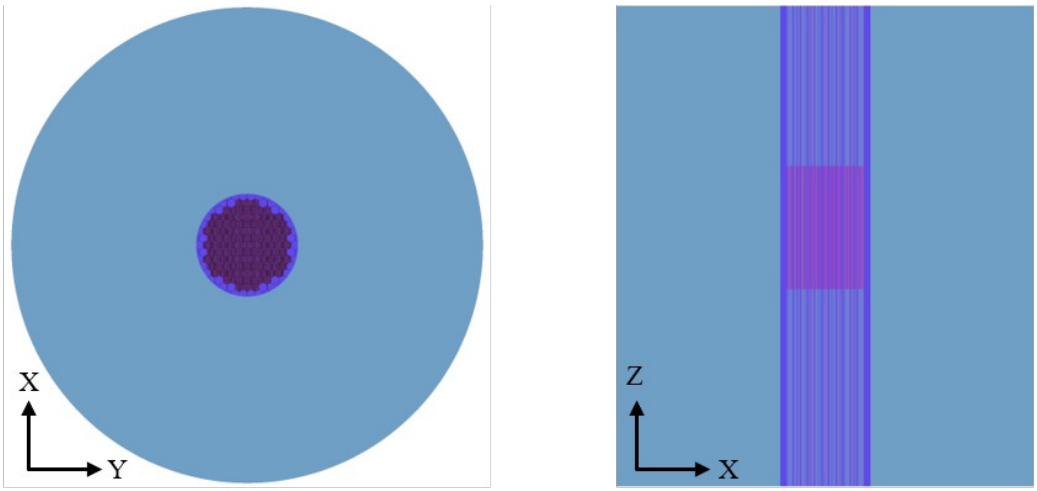

Figure 4. The X-Y and X-Z sections of the reactor

The fuel rod is a simplified model consisting of fuel pellets, air gap and cladding, with a total length of 50 cm. The fuel assembly has a hexagonal design and contains 91 fuel rods. The geometry of the fuel rod and the fuel assembly are shown in Figure 5. The detailed parameters of the high flux reactor are given in Table 1.

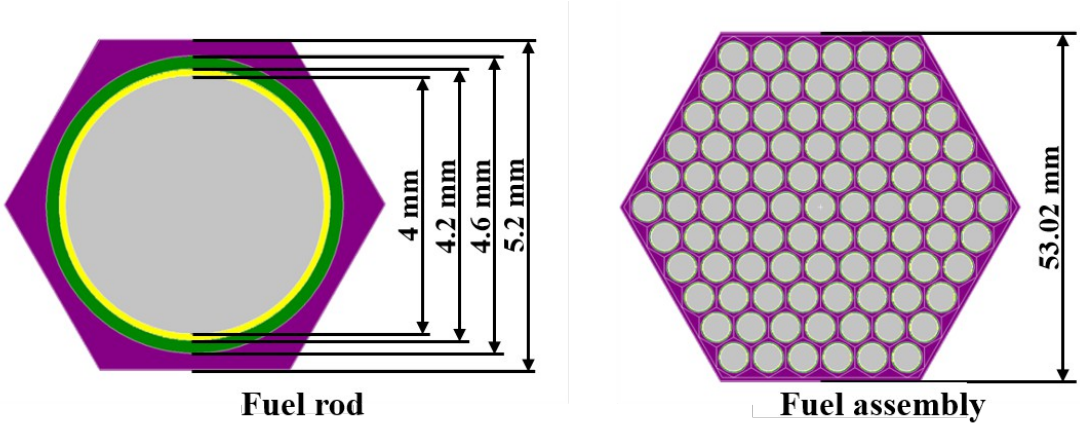

Figure 5. The geometry of the fuel rod and the fuel assembly

Table 1. The detailed parameters of the high flux reactor

Parameters	Value
Thermal power	150 MW
Loading capacity of Fuel / U-235	779 /175.3 kg
Equivalent diameter of active zone	58.14 cm
Height of active zone	50 cm

Average line power density	302.45 W/cm
Maximum line power density	404.20 W/cm
Average volume power density	1130 W/cm^3
Fuel material	U-10%Zr alloy
Enrichment of ^{235}U	25 %
Inner / outer diameter of fuel rod	4 / 4.6 mm
Filled gas in the gaps	Helium
Fuel rod clearance width	0.1 mm
Cladding material	T91
Thickness of the cladding	0.2 mm
Ratio of pitch to diameter (P/D)	1.1304
Number of assembly	109
Number of fuel rods per assembly	91
Axial / radial thickness of reflector layers	80 / 120 cm

The target for producing Cf-252 is a mixture of plutonium, americium and curium [9], and the nuclide composition of the target is shown in Table 2. The target is irradiated for five cycles, and each cycle consists of a 25-day irradiation. This target irradiation is representative of typical operations during a californium production campaign.

Table 2. The nuclide composition of the target for producing Cf-252

Nuclide	Weight	Nuclide	Weight
Pu-238	0.002 g	Cm-244	8.734g
Pu-239	0.001 g	Cm-245	0.271g
Pu-240	0.565 g	Cm-246	22.349g
Pu-242	0.016 g	Cm-247	0.647g
Am-243	3.903g	Cm-248	4.743g

2.2 Production Evaluation by Monte Carlo Burnup Calculation

The yields of transplutonium isotopes can be obtained by performing the Monte Carlo burnup calculation, which is the coupling of the Monte Carlo criticality calculation and the burnup calculation. Figure 6 gives the flowchart for evaluating the transplutonium isotopes production by the Monte Carlo burnup calculation.

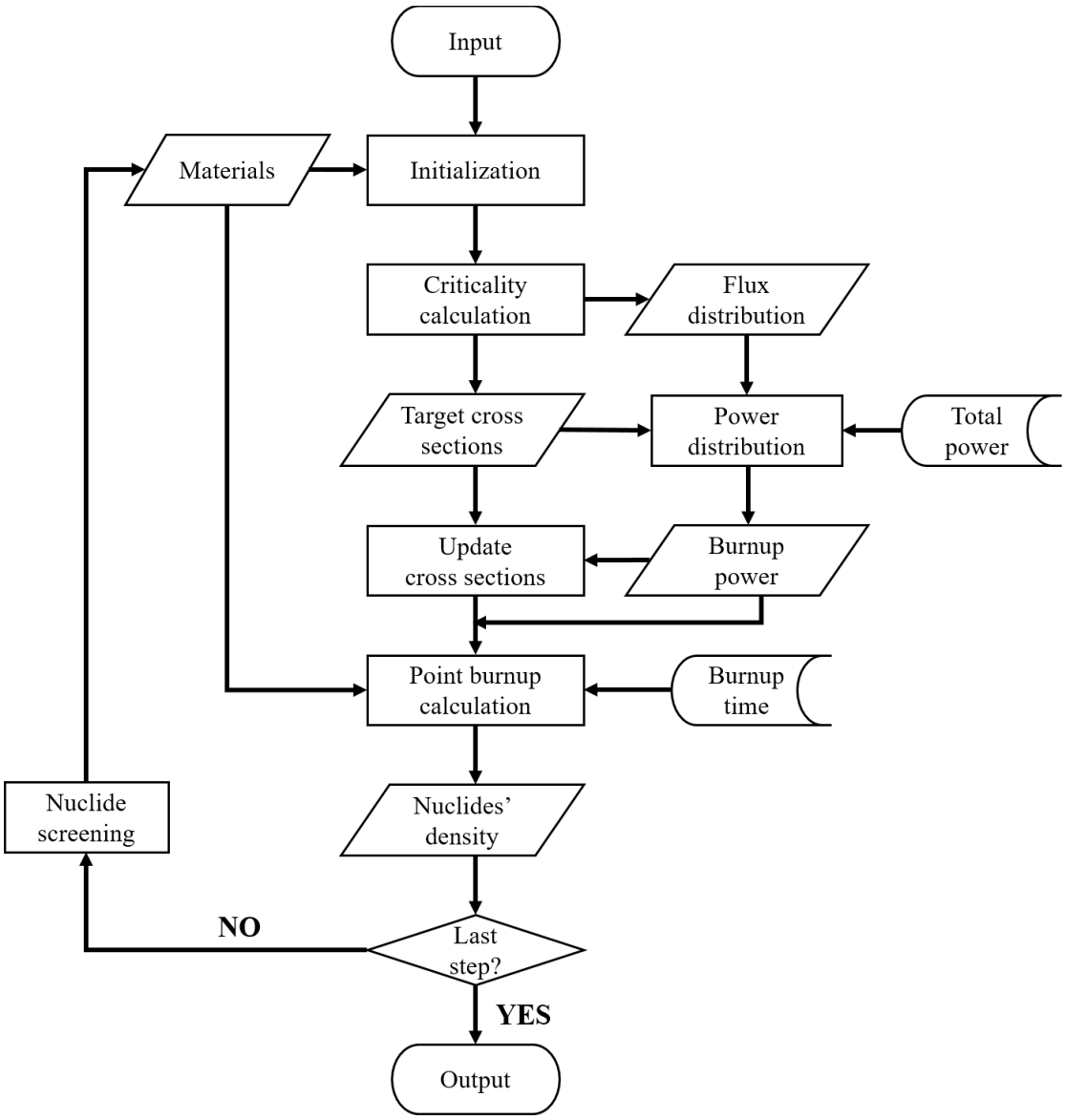

Figure 6. Flowchart for evaluating production by Monte Carlo burnup calculation.

The point burnup equation describes the nuclides' transmutation with time when the target is irradiated in a high-flux reactor. For each nuclide in the burnup chain, its time-dependent point burnup equation can be written as

, (1)

where n_i is the density of the i^{th} nuclide, λ_i^{eff} is the effective decay constant of the i^{th} nuclide, and $b_{i,j}^{eff}$ is the branching ratio for transmutation of the i^{th} nuclide to the j^{th} nuclide. λ_i^{eff} and $b_{i,j}^{eff}$ can be calculated from the following formula,

, (2)

where λ_i is the decay constant of the i^{th} nuclide, ϕ is the neutron flux, and $\sigma_{i,j}$ is the one-group cross section where the i^{th} nuclide's reaction generates the j^{th} nuclide.

During the burnup calculation, the one-group cross section and neutron flux within each burnup step are assumed to be constant so that the point burnup equation can be treated as a first-order linear ordinary differential equation. Writing it into a matrix form, we have the following more concise expression,

, (3)

where matrix **A** represents the coefficient matrix of the N order point burnup equation, which is regarded as a constant matrix in a single burnup step.

Given the initial boundary conditions, the solution of Equation (3) can be written in the form of an exponential matrix,

, (4)

where matrix **A***t* is referred to as the burnup matrix for the convenience of quotation.

Because of the extremely low yields of transplutonium isotopes and the complex nuclide composition of the target, the point burnup model usually adopts a complex nuclide system, which needs to cover more than a thousand isotopes, including a large number of short half-life nuclides. For example, the ORIGEN-S burnup database [35] contains about 1,500 nuclides. Some of these nuclides, such as Po-212, have a half-life of 10^{-7}s. Therefore, the point burnup equations of transplutonium isotopes production are not only large in number but also rigid, which brings difficulties to its solution.

As shown in Equation (2), the cross section of the target is required for the Monte Carlo burnup equation, so the criticality calculation should be performed. The k-eigenvalue neutron transport equation can be written as [36]

, (5)

where L represents the leakage operator, C represents the collision operator, S

represents the scattering operator, M represents the fission operator, $k$eff represents the effective multiplication factor, and ϕ is the neutron flux.

Physical parameters around the target, such as the neutron flux, fission reaction rate and absorption reaction rate, can be obtained by solving Equation (5). The Monte Carlo method has the following formula for calculating reaction rates,

, (6)

where $\sum_g$ represents the macroscopic cross section in the g^{th} energy interval, and $\sum$ represents nuclides' cross section related to position r and energy E.

Therefore, we have the following formula for calculating the cross section needed by Monte Carlo burnup calculation,

(7)

The above formulas show that the Monte Carlo burnup calculation is complex and costly [37-38]. Tested in the high flux reactor shown in Figure 4, with the calculation parameters of 1,000,000 neutrons per cycle, 100 inactive cycles, 300 active cycles and 10 burnup steps, it takes 150 minutes to perform one Monte Carlo burnup calculation with 64 threads on the 2nd Gen AMD EPYC™ 7742. Even though only considering the production of Cf-252, Cm-244, Cm-242 and Pu-238, and only analyzing the five design parameters (shown in Figure 9), a total of 9720 calculations are needed, with a computing time of 1458,000 minutes (1012.5 days). This amount of computation time is unacceptable.

Moreover, since the Monte Carlo burnup calculation only needs the one-group cross section, the calculations can only give the influence of the whole neutron spectrum on the production efficiency, not a closer analysis of each single energy interval. So when optimizing the neutron spectrum, we can only from the macroscopic design parameters, cannot know which energy intervals are favorable and which are unfavorable to production, and thus cannot provide more detailed guidance for the optimization.

Therefore, we need to grasp the physical nature of the production process and

find a new rapid diagnosis method which can simplify the calculation and analyze the production process in more detail. A rapid diagnosis method is helpful for evaluating, screening and optimizing the irradiation scheme.

2.3 Rapid Diagnosis Method Based on SEIV and ESTV

The root cause of the low production of transplutonium isotopes is fission loss [14]. When the target is irradiated in a high flux reactor, the target material changes from nuclides with a small mass number to nuclides with a large mass number through absorption reactions. Besides the absorption reaction, the fission reaction also occurs. Once the fission reaction occurs, the production of transplutonium isotopes is stopped, causing fission losses and leading to a low conversion rate. Therefore, the ratio of absorption rate to fission rate (A/F) is an important physical quantity affecting production efficiency. The production efficiency can be assessed by analyzing the A/Fs of the nuclides in the nuclide chain. Moreover, the A/F can be calculated in individual energy intervals, thus achieving refined Neutronics analysis. Taking the production of Cf-252 from the target described in Table 2 as an example, Figure 7 shows the A/Fs of the intermediate nuclides, Cm-244, Cm-245, Cm-246, Cm-247, Cm-248, Bk-249, Cf-250 and Cf-251. The nuclear data comes from JANIS [39].

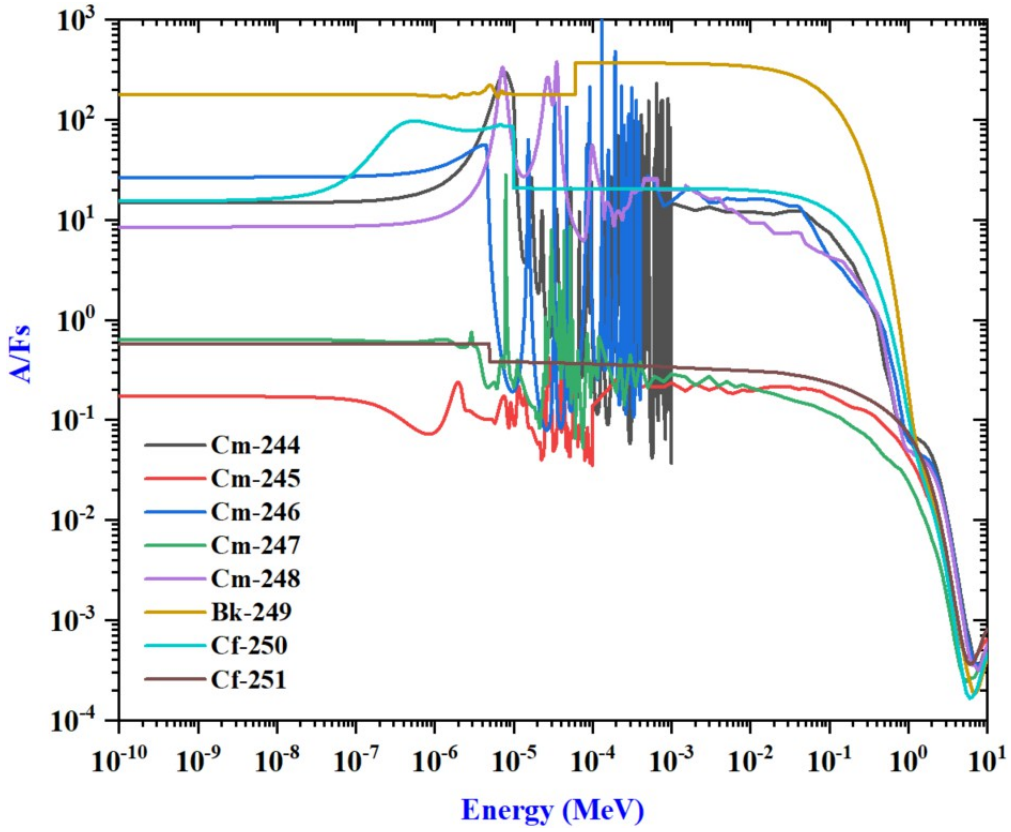

Figure 7. The A/Fs of the intermediate nuclides for producing Cf-252

As shown in Figure 7, the A/Fs of different nuclides vary greatly, and so do the A/Fs of different energy intervals, so different nuclides and different energy intervals have significantly different effects on production efficiency. It is not accurate to only analyze the whole energy spectrum, and a more detailed analysis of each energy interval is needed.

A rapid diagnosis method based on the neutron spectrum around the target is proposed to realize the rapid and refined evaluation of the different production schemes. The model only needs to obtain the neutron spectrum around the target by the Monte Carlo criticality calculation [40-41] to evaluate the efficiency of different production schemes, avoiding the burnup calculation and greatly reducing the required computing resources. Therefore, the rapid diagnosis method can screen out the optimal scheme for transplutonium isotopes production quickly, and helps provide direction for optimizing the irradiation scheme.

The model is divided into four steps: 1) the neutron spectrum around the target is

obtained after the Monte Carlo criticality calculation, which can be described by the 46-group neutron flux, the 46-group fission rate and the 46-group absorption rate, 2) define the physical quantity "Single Energy Interval Value (SEIV)", and calculate the SEIV of these 46 energy intervals, 3) define the physical quantity "Energy Spectrum Total Value (ESTV)", and use the 46-group neutron flux and the 46-group SEIV to calculate the ESTV of the neutron spectrum, and 4) evaluate the efficiency of different schemes by comparing the ESTV. Those with higher ESTV are considered to have higher production efficiency and yield. The schematic diagram is shown in Figure 8.

The Single Energy Interval Value (SEIV) is calculated by

, (8)

where the subscript "i" represents the serial number of energy intervals, $R_{a,i}$ represents the absorption rate in the i^{th} energy interval, $R_{f,i}$ represents the fission rate in the i^{th} energy interval, ϕ_i represents the neutron flux in the i^{th} energy interval.

The SEIV is the product of two expressions. The first is the A/F, indicating whether it tends to undergo an absorption or a fission reaction within this energy interval. The other is the ratio of the absorption rate to the neutron flux, which indicates the probability of the absorption reaction occurring in this energy interval. Therefore, a higher SEIV means that within this energy interval, absorption reactions tend to occur rather than fission reactions, and more absorption reactions occur. The energy interval with a high SEIV is considered important in the production process, and the neutron flux in this energy interval should be increased as much as possible.

The Energy Spectrum Total Value (ESTV) is calculated by

. (9)

The ESTV is the integral value of SEIV along with the neutron spectrum, indicating the target nuclide's overall trend of absorbing neutrons without fission. We believe that the production scheme with higher ESTV produces transplutonium isotopes more efficiently. The ESTV is only related to the neutron spectrum around the target, and the burnup calculation is no more needed, so the ESTV can be used for

the rapid evaluation of the production scheme.

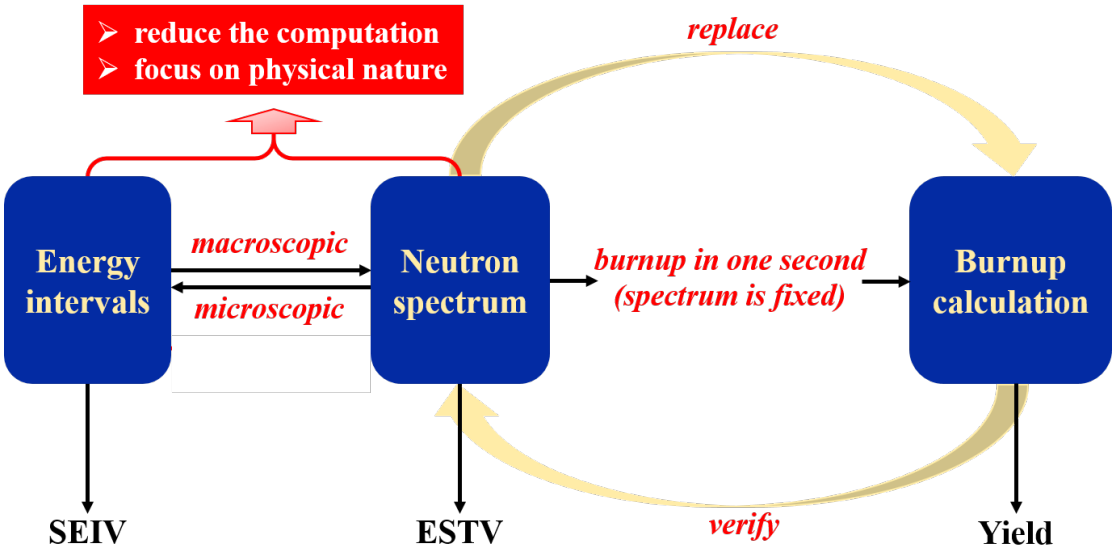

Figure 8. The schematic diagram of the rapid diagnosis method

3. NUMERICAL AND EXPERIMENTAL VERIFICATION

3.1 Numerical Verification

The rapid diagnosis method is verified by comparing the burnup calculation with the ESTV. We optimize the production efficiency by adjusting the following five design parameters: 1) the selection of the moderator, 2) the layout of the moderator, 3) the position of the target, 4) the size of the target, and 5) the shape of the target. The optional values for these five design parameters are shown in Figure 9.

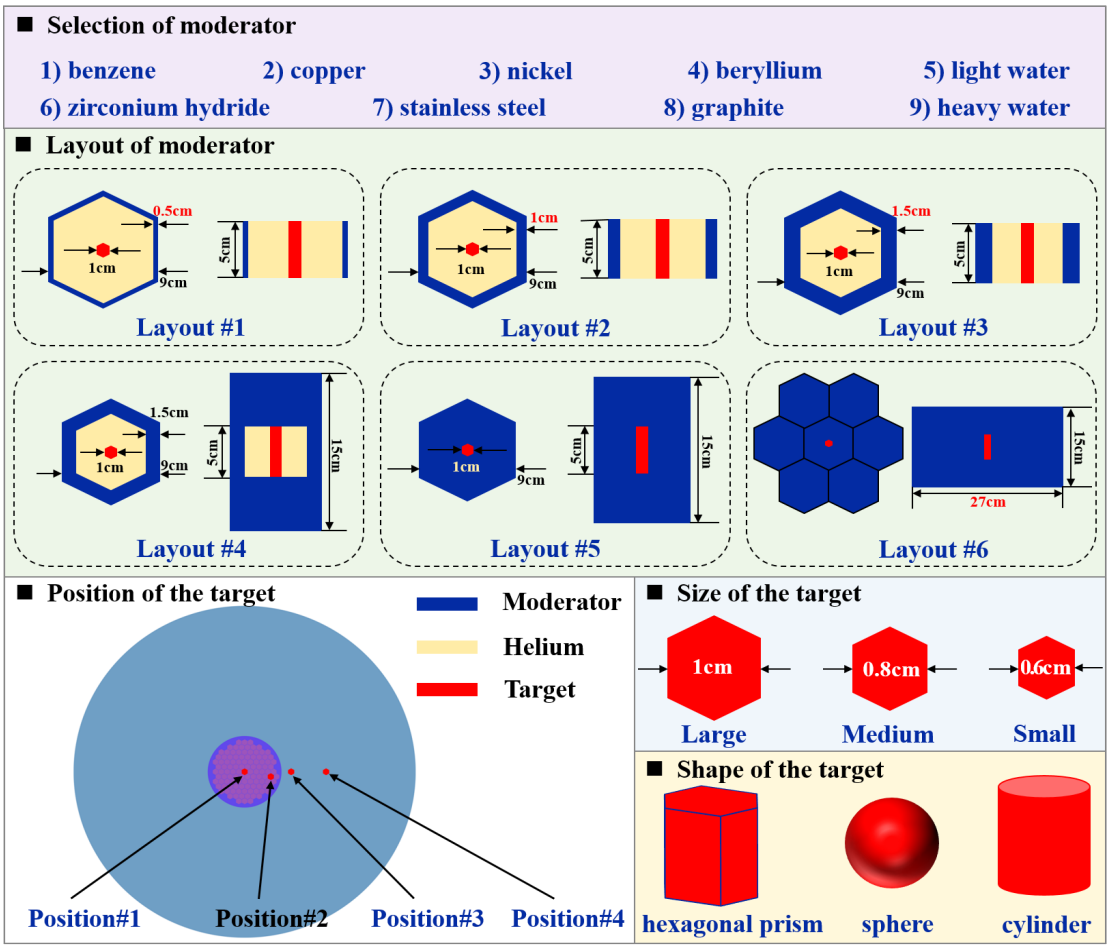

Figure 9. The optional values for these five design parameters

We use a large hexagonal prism target with Position #1 as the initial scheme, and zirconium hydride is selected as the moderator. Different irradiation schemes are obtained by modifying the layout of the moderator. We perform criticality calculations to obtain the neutron spectrum around the target. The SEIV and ESTV are determined and used to evaluate the efficiency of the irradiation schemes.

We take Pu-238, Cm-242, Cm-244, and Cf-252 as examples. The target for producing Pu-238 is Np-237. The target for producing Cm-242 is Am-241. The target for producing Cm-244 is Pu-239. The nuclide composition of the target for producing Cf-252 is shown in Table 2. The SEIV and ESTV for the target without the moderator (bare target) and the six layouts of the moderator are calculated, so there are seven production schemes for each transplutonium isotope to be produced. The SEIV for producing these four transplutonium isotopes is given in Table 3. The ESTV for

producing these four transplutonium isotopes is given in Table 4.

As shown in Table 3, the optimal neutron spectrum for producing Pu-238, Cm-242, Cm-244 and Cf-252 is not always the softer, the better. The energy interval [4.14E-07 MeV, 8.76E-06 MeV] has the highest SEIV for producing Pu-238. The energy interval [1E-11 MeV, 1E-07 MeV] has the highest SEIV for producing Cm-242. The energy interval [1E-07 MeV, 4.14E-07 MeV] has the highest SEIV for producing Cm-244. The energy interval [8.76E-07, 1.86E-06] has the highest SEIV for producing Cf-252. Moreover, the SEIV varies greatly in different energy intervals. For example, the maximum deviation of the SEIV in different energy intervals can be up to 1.37×10^{9} times for producing Cf-252. Therefore, the efficiency of transplutonium isotopes can be improved by modifying the neutron spectrum around the target [42-43].

As shown in Table 4, the ESTV varies greatly for different irradiation schemes. For example, the maximum deviation of the ESTV can be up to 21.3 times for producing Cf-252. Moreover, the bare target always has the lowest ESTV regardless of the isotope produced. So the production of transplutonium isotopes requires placing a moderator around the target. Layout #6 of the moderator has the highest ESTV for producing Pu-238, Cm-242, Cm-244, and Layout #5 has the highest ESTV for producing Cf-252. Since the SEIV and ESTV can be used to analyze the production efficiency of each energy interval in detail, the SEIV and ESTV are helpful in providing direction for optimizing the irradiation scheme.

Table 3. SEIV for producing Pu-238, Cm-242, Cm244 and Cf-252

Energy / MeV	Pu-238	Cm-242	Cm-244	Cf-252
[1.00E-11, 1.00E-07]	4.55E+04	3.06E+03	4.96E+00	2.42E+00
[1.00E-07, 4.14E-07]	2.78E+04	2.10E+03	1.10E+01	2.53E+00
[4.14E-07, 8.76E-07]	6.99E+04	1.88E+03	9.02E-01	1.75E+01
[8.76E-07, 1.86E-06]	1.93E+04	4.87E+02	7.34E-02	1.16E+02
[1.86E-06, 5.04E-	3.89E+03	3.17E+02	1.89E-02	1.48E+00

06]				
[5.04E-06, 1.07E-05]	6.12E+03	1.13E+02	1.17E-01	9.41E+00
[1.07E-05, 3.73E-05]	1.50E+03	1.24E+02	2.15E-01	4.46E+00
[3.73E-05, 1.01E-04]	2.48E+02	1.21E+02	1.52E-01	1.91E+00
[1.01E-04, 2.14E-04]	1.48E+02	1.78E+02	1.70E-01	1.90E+00
[2.14E-04, 4.54E-04]	1.61E+02	1.34E+02	2.62E-01	1.90E+00
[4.54E-04, 1.58E-03]	1.55E+02	7.46E+01	1.16E-01	1.73E+00
[1.58E-03, 3.35E-03]	7.21E+01	4.83E+01	1.19E-01	7.63E-01
[3.35E-03, 7.10E-03]	4.26E+01	2.64E+01	8.62E-02	5.65E-01
[7.10E-03, 1.50E-02]	2.62E+01	2.02E+01	3.31E-02	4.08E-01
[1.50E-02, 2.19E-02]	1.89E+01	1.61E+01	1.62E-02	3.14E-01
[2.19E-02, 2.42E-02]	1.65E+01	1.41E+01	1.36E-02	2.83E-01
[2.42E-02, 2.61E-02]	1.56E+01	1.35E+01	1.15E-02	2.67E-01
[2.61E-02, 3.18E-02]	1.50E+01	1.32E+01	9.06E-03	2.46E-01
[3.18E-02, 4.09E-02]	1.22E+01	1.33E+01	6.17E-03	2.12E-01
[4.09E-02, 6.74E-02]	8.42E+00	1.05E+01	3.88E-03	1.49E-01
[6.74E-02, 1.11E-01]	4.25E+00	6.26E+00	2.01E-03	7.85E-02
[1.11E-01, 1.83E-01]	1.71E+00	3.22E+00	1.48E-03	4.19E-02
[1.83E-01, 2.97E-01]	5.54E-01	1.31E+00	1.19E-03	2.19E-02
[2.97E-01, 3.69E-01]	1.89E-01	4.81E-01	8.20E-04	1.34E-02
[3.69E-01, 4.98E-01]	4.20E-02	2.08E-01	4.86E-04	7.76E-03
[4.98E-01, 6.08E-01]	8.78E-03	7.30E-02	2.75E-04	3.71E-03
[6.08E-01, 7.43E-01]	3.46E-03	2.23E-02	1.48E-04	1.85E-03
[7.43E-01, 8.21E-01]	1.85E-03	7.91E-03	6.30E-05	1.12E-03
[8.21E-01, 1.00E+00]	1.23E-03	4.01E-03	2.94E-05	7.19E-04

[1.00E+00, 1.35E+00]	5.54E-04	1.45E-03	1.12E-05	4.20E-04
[1.35E+00, 1.65E+00]	2.45E-04	6.23E-04	4.44E-06	3.30E-04
[1.65E+00, 1.92E+00]	1.39E-04	3.14E-04	2.50E-06	2.82E-04
[1.92E+00, 2.23E+00]	9.06E-05	1.39E-04	1.43E-06	1.93E-04
[2.23E+00, 2.35E+00]	6.45E-05	7.85E-05	9.42E-07	1.35E-04
[2.35E+00, 2.37E+00]	5.95E-05	6.54E-05	8.18E-07	1.20E-04
[2.37E+00, 2.47E+00]	5.53E-05	5.63E-05	7.20E-07	1.10E-04
[2.47E+00, 2.73E+00]	4.52E-05	3.94E-05	5.13E-07	8.03E-05
[2.73E+00, 3.01E+00]	3.26E-05	2.00E-05	3.04E-07	4.89E-05
[3.01E+00, 3.68E+00]	2.31E-05	7.95E-06	1.85E-07	2.09E-05
[3.68E+00, 4.97E+00]	1.18E-05	1.17E-06	1.10E-07	3.64E-06
[4.97E+00, 6.07E+00]	5.27E-06	1.05E-07	3.67E-08	4.23E-07
[6.07E+00, 7.41E+00]	2.35E-06	1.77E-08	4.22E-09	1.37E-07
[7.41E+00, 8.61E+00]	1.17E-06	9.91E-09	4.80E-09	8.47E-08
[8.61E+00, 1.00E+01]	7.86E-07	1.13E-08	2.56E-08	8.52E-08
[1.00E+01, 1.22E+01]	5.51E-07	0.00E+00	1.19E-07	8.78E-08
[1.22E+01, 1.42E+01]	0	6.32E-09	1.32E-07	0

Table 4. ESTV for producing Pu-238, Cm-242, Cm244 and Cf-252

Schemes	Pu-238	Cm-242	Cm-244	Cf-252
Bare target	4.50E-03	5.64E-03	3.92E-06	9.22E-05
Layout#1	1.36E-01	1.92E-02	2.55E-05	4.41E-04
Layout#2	6.78E-01	4.05E-02	5.00E-05	1.08E-03
Layout#3	1.60E+00	7.14E-02	7.59E-05	1.72E-03
Layout#4	5.46E+00	1.74E-01	1.77E-04	4.39E-03
Layout#5	6.26E+00	1.99E-01	2.01E-04	4.94E-03

Layout#6	1.11E+01	2.94E-01	2.42E-04	4.59E-03

It is not rigorous to compare the different irradiation schemes only by the SEIV and ESTV, so we need to verify this method. To verify the effectiveness of the rapid diagnosis method, we perform the burnup calculations with RMC code [44] to calculate the yields of Pu-238, Cm-242, Cm-244, and Cf-25, respectively. Since the neutron spectrum is changing during the burnup process, we first simulate the one-second burnup process to ensure that the neutron spectrum used to calculate the ESTV is consistent with the neutron spectrum used to calculate the yields. In the one-second burnup process, we can clarify the relationship between the ESTV and the yields with a fixed neutron spectrum. The yields in one second for Pu-238, Cm-242, Cm244 and Cf-252 are given in Table 5.

Table 5. Yields in one second for Pu-238, Cm-242, Cm244 and Cf-252 (/g)

Schemes	Pu-238	Cm-242	Cm-244	Cf-252
Bare target	5.03E-13	1.53E-12	1.68E-45	1.94E-37
Layout#1	1.07E-12	2.29E-12	4.96E-45	6.90E-37
Layout#2	1.86E-12	4.20E-12	1.07E-44	1.32E-36
Layout#3	2.86E-12	6.75E-12	1.92E-44	1.79E-36
Layout#4	6.78E-12	1.62E-11	2.44E-43	1.38E-35
Layout#5	7.62E-12	1.80E-11	2.85E-43	1.46E-35
Layout#6	1.05E-11	2.64E-11	1.60E-43	5.79E-36

As shown in Table 5, no matter which isotope is produced, the yield in one-second increases with the increases of the ESTV. Therefore, the ESTV can be used to evaluate the yield with the same neutron spectrum. However, the one-second burnup can only describe the physical process at the early stage of irradiation but cannot describe the entire irradiation cycle. To ensure whether the ESTV can indicate the yield of the whole irradiation cycle, the burnup process of the target irradiation for 90 days is also simulated. The yields in 90 days for Pu-238, Cm-242, Cm244 and Cf-252 are given in Table 6.

Table 6. Yields in 90 days for Pu-238, Cm-242, Cm244 and Cf-252 (/g)

Schemes	Pu-238	Cm-242	Cm-244	Cf-252
Bare target	1.65E+00	1.28E+00	1.96E-02	7.95E-03
Layout#1	3.03E+00	1.74E+00	4.51E-02	2.07E-02
Layout#2	4.64E+00	2.68E+00	7.91E-02	3.42E-02
Layout#3	6.07E+00	3.58E+00	2.98E-01	4.20E-02
Layout#4	9.44E+00	6.57E+00	1.00E+00	8.23E-02
Layout#5	1.01E+01	7.08E+00	7.08E+00	9.80E-02
Layout#6	1.16E+01	1.05E+01	1.05E+01	8.30E-02

As shown in Table 6, no matter which isotope is produced, the yield in 90 days increases with the increase of the ESTV. Therefore, the ESTV can not only indicate the production efficiency at the early stage but also indicate the efficiency of the whole irradiation cycle. So the rapid diagnosis method based on the SEIV and ESTV can be used to evaluate the efficiency of transplutonium isotopes production.

3.2 Experimental Verification

Since the high flux reactor shown in Figure 4 has yet to be built, experimental studies cannot be carried out on this reactor, so the experimental verification of the rapid diagnosis method is carried out on the High Flux Isotope Reactor (HFIR) [45]. HFIR has been producing Cf-252 since 1966 and currently accounts for 70% of the world's supply of Cf-252, so HFIR has a large number of measured data in transplutonium isotopes production.

Rated at 100 MW and currently operating at 85 MW, HFIR has the world's

highest steady-state neutron heat flux (2.6×10^{15} $cm^{-2}\cdot s^{-1}$). HFIR is a light-water-cooled moderated flux trap reactor using highly enriched U-235. The reactor core consists of many concentric annular zones, each about 61 cm high (the fuel height is 51 cm). At the center is a 12.70 cm cylindrical pore called “neutron flux trap”, containing 37 vertical experimental holes. The neutron flux trap is surrounded by two concentric fuel assemblies. The reactor core and neutron flux trap are shown in Figure 10 [46].

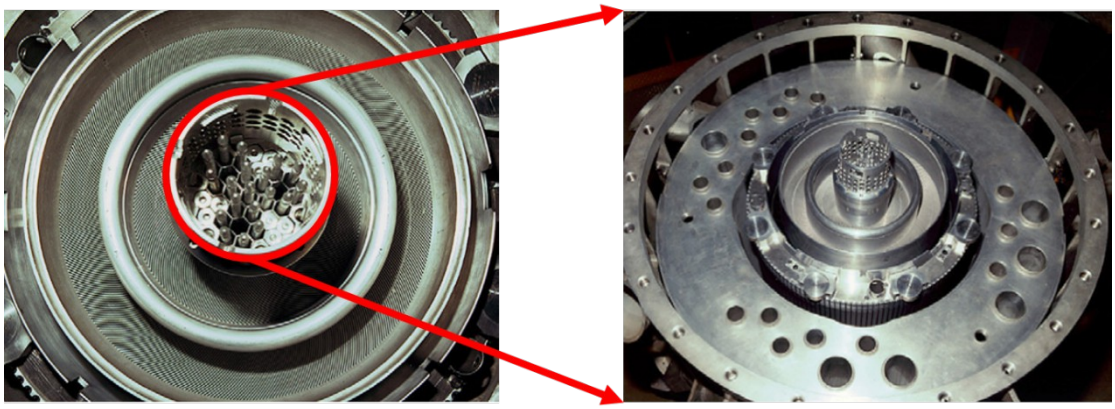

Figure 10. The reactor core and neutron flux trap of HFIR

Because the rapid diagnosis method uses the ESTV to evaluate the production efficiency of different irradiation schemes, the Monte Carlo criticality calculation should be performed to calculate the ESTV. RMC code is used to model HFIR, and the input card of HFIR is given in the attachment. See Figure 11 for the core modeling and the neutron flux trap modeling.

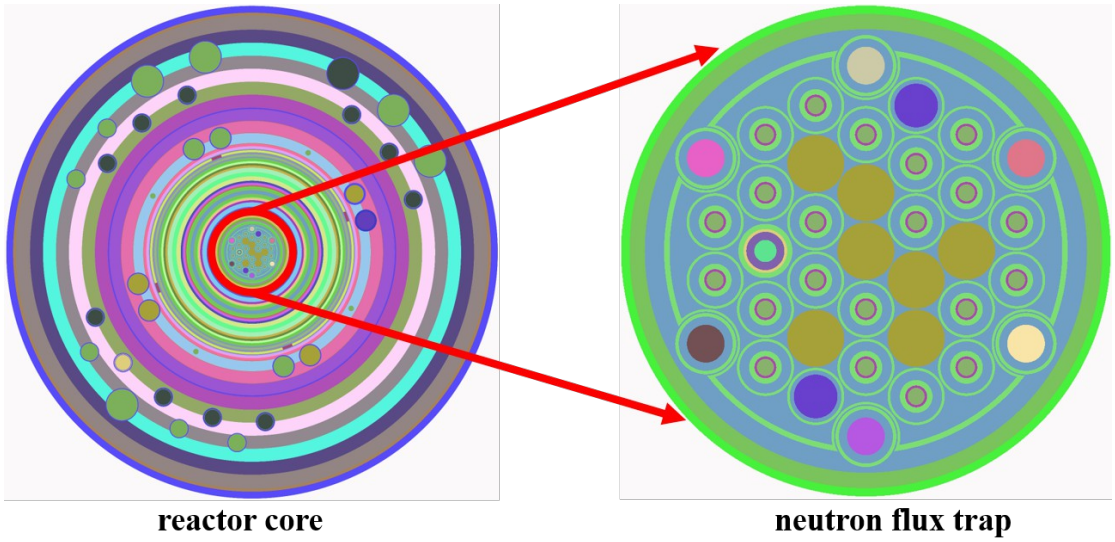

Figure 11. The core modeling and the neutron flux trap modeling of RMC code

To verify the correctness of the modeling, the radial distributions of thermal neutron flux and total neutron flux are calculated and compared with reference solutions, as shown in Figure 12. It shows that the flux distributions calculated by RMC are in good agreement with the reference solutions, which proves the correctness of the HRIR modeling.

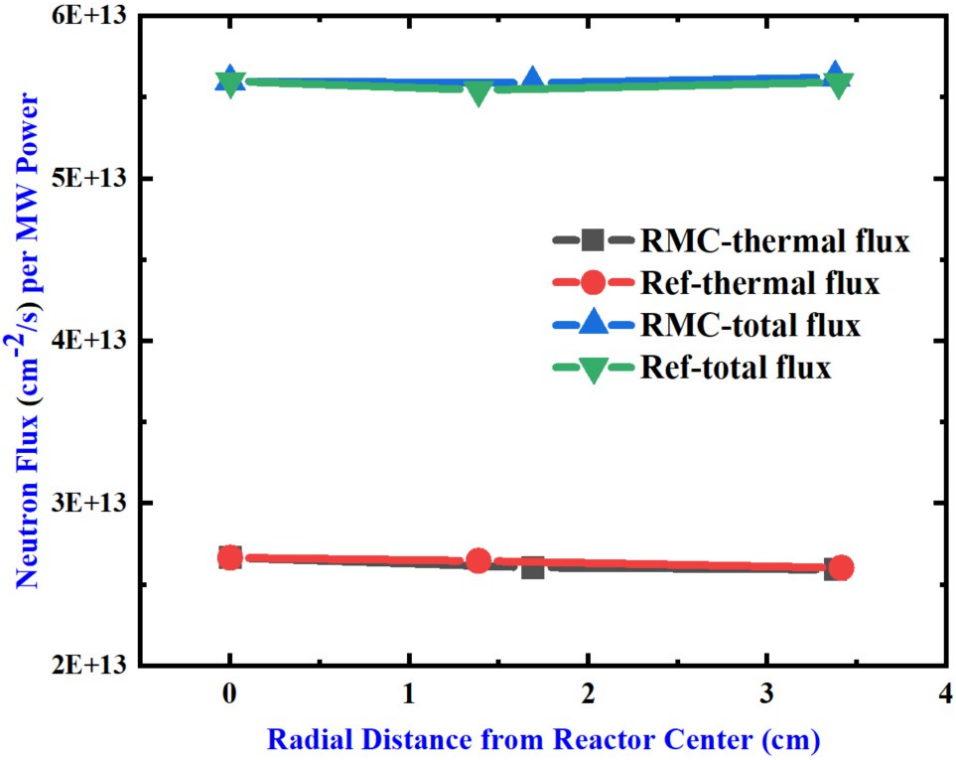

Figure 12. Comparison of the radial flux distributions

Then experimental verification is carried out. The target design shown in Figure 13 was irradiated in HFIR for five days. Four irradiation schemes were formed with two target nuclide compositions and two irradiated positions, namely, ^{245}Cm_A, ^{245}Cm_C, Cf_A, and Cf_C. The yields of heavy nuclei (all nuclides heavier than the nuclides in the target) for the four irradiation schemes were measured [9], and the corresponding ESTV was calculated. The experimental results are shown in Table 7.

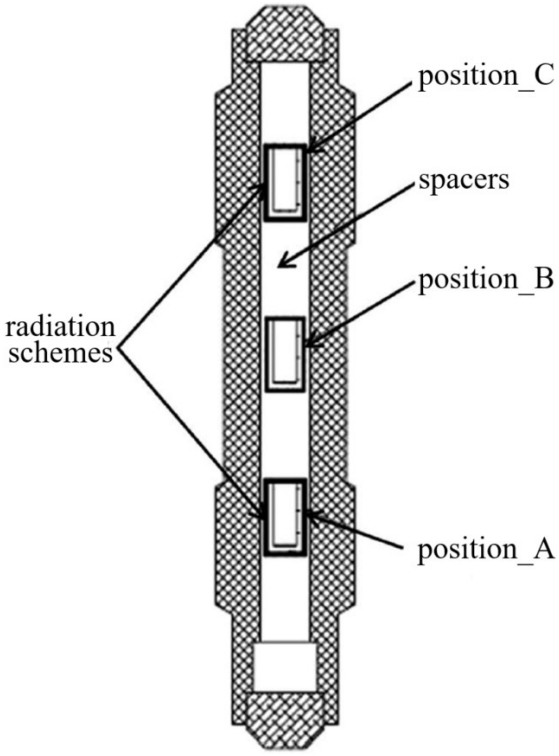

Figure 13. Experimental target design

Table 7. Results of experimental verification

Irradiation schemes	Nuclide composition of the target	Irradiation duration	Yields of heavy nuclei (experiments)	ESTV (simulations)
^{245}Cm_A	^{245}Cm: 45.9±0.3ng	5 days	7.861 ng	1.00E-12
^{245}Cm_C	^{249}Cf: 0.099±0.001ng		9.308 ng	1.09E-12
Cf_A	^{249}Cf: 42.4±0.3ng ^{250}Cf: 11.3±0.2ng	5 days	12.6 ng	3.23E-11
Cf_C	^{251}Cf: 30.2±0.5ng		12.7 ng	3.50E-11

Because the target nuclide composition should be the same when comparing the ESTV of different irradiation schemes, we compared 245Cm_A with 245Cm_C and Cf_A with Cf_C, respectively. As shown in Table 7, the measured yield of heavy nuclei of ^{245}Cm_A is lower than that of ^{245}Cm_C, and the corresponding ESTV of ^{245}Cm_A is also lower than that of ^{245}Cm_C. Meanwhile, the measured yield of heavy nuclei of Cf_A is lower than that of Cf_C, and the corresponding ESTV of the Cf_A is also lower than that of Cf_C. The experimental results satisfy the law in the rapid

diagnosis method that the higher the ESTV is, the higher the production efficiency is. Therefore, the experimental verification proves the correctness of the rapid diagnosis method.

In the next chapter, we will use the rapid diagnosis method to realize the rapid screening and determination of the optimal irradiation scheme.

4. SENSITIVITY ANALYSIS AND OPTIMIZATION APPLICATION

4.1 The Logic of Optimization

There are five design parameters to be optimized: 1) the selection of the moderator, 2) the layout of the moderator, 3) the position of the target, 4) the size of the target, and 5) the shape of the target.

As shown in Table 3, no matter which isotope is produced, the energy interval

with the highest SEIV is always in the thermal range, so we need to arrange the moderator to soften the neutron spectrum around the target. We hope to select the material with the strongest moderating power as the moderator so that we can achieve the best neutron spectrum by deploying the least amount of moderator. The moderating power of various materials is the inherent property of the material and is not affected by other design parameters, so the moderator material can be determined first. We use a large hexagonal prism target with Layout #1 and Position #1 as the initial scheme. Nine moderator materials are tested, and the neutron spectrums around the target are tallied, as shown in Figure 14.

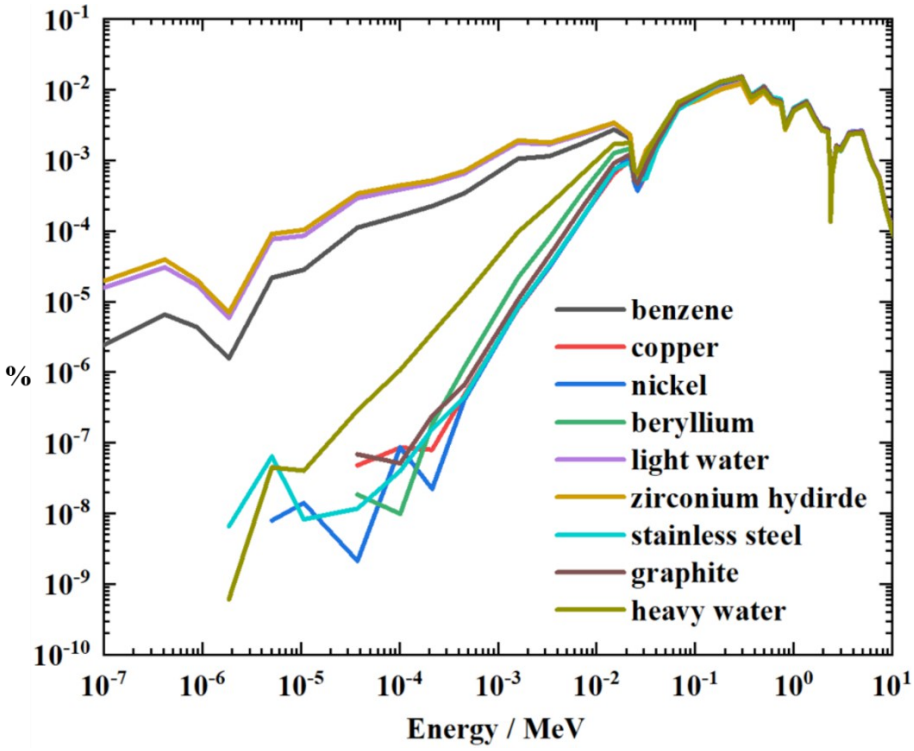

Figure 14. Neutron spectrums with different moderators

As shown in Figure 14, zirconium hydride has the best moderating power, so zirconium hydride is selected as the moderator, and the moderator selection will not be considered in all subsequent analyses.

To determine an optimal production scheme, we have to decide the optimal design parameter for the layout of the moderator, the position, size and shape of the target. We use a large hexagonal prism bare target with Position #1 as the initial

scheme and then optimize the four design parameters. The optimization order of these four parameters is important. We determine the optimization order by sensitivity analysis. The sensitivity coefficient of a design parameter d to production efficiency is defined as

$$\text{,} \qquad (10)$$

where P represents the production efficiency, d represents a design parameter.

So the sensitivity coefficient is positively correlated with the ESTV's maximum increase that can be obtained by adjusting a design parameter. The larger the maximum increase, the more important this design parameter is to the optimization process, so we optimize it first. After one of these design parameters is optimized, we take the optimized scheme as the starting scheme to optimize the remaining design parameters, and so on, until all design parameters are optimized. A logical diagram of the optimization process is shown in Figure 15. This paper takes Cf-252 as an example to describe the optimization process of the irradiation scheme in detail. The optimal schemes for Pu-238, Cm-242 and Cm-244 will be given in Section 3.6.

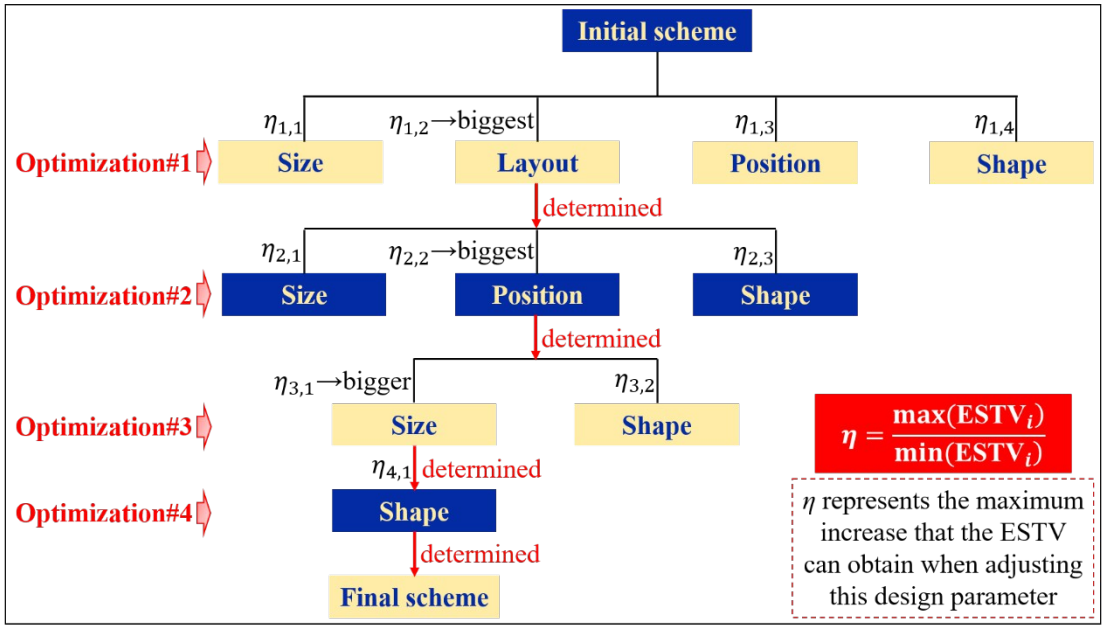

Figure 15. The diagram of optimization logic

4.2 First Round Sensitivity Analysis and Optimization

The first round of sensitivity analysis and optimization needs to consider four design parameters, i.e., the layout of the moderator, the position, size and shape of the

target. The optional values for the four design parameters are shown in Figure 9. New irradiation schemes can be obtained by adjusting one of the four design parameters based on the initial scheme. The ESTVs for all new schemes are shown in Table 8, and the symbol "η" represents the sensitivity coefficient.

Table 8. The ESTVs for the first round optimization

Layout	ESTV	Position	ESTV
bare target	9.22E-05	Position#1	9.22E-05
Layout#1	4.41E-04	Position#2	1.07E-04
Layout#2	1.08E-03	Position#3	5.43E-04
Layout#3	1.72E-03	Position#4	6.97E-04
Layout#4	4.39E-03		
Layout#5	4.94E-03		
Layout#6	4.59E-03		
η_L	**53.6**	η_P	**7.56**
Shape	ESTV	Size	ESTV
hexagonal prism	9.22E-05	large	9.22E-05
sphere	9.78E-05	medium	9.35E-05
cylinder	9.22E-05	small	9.22E-05
η_{Sh}	**1.06**	η_{Si}	**1.01**

As shown in Table 8, the layout of the moderator can improve the ESTV the most, so the layout of the moderator should be optimized first. Moreover, Layout#5 has the highest ESTV, so the layout of the moderator is selected as Layout #5. After the first round of optimization, the scheme becomes a large hexagonal prism target with Position #1 and Layout #5.

4.3 Second Round Sensitivity Analysis and Optimization

The second round of sensitivity analysis and optimization needs to consider three design parameters, i.e., the position, size and shape of the target. All new irradiation

schemes are obtained based on the scheme after the first round of optimization. The ESTVs for the second round of optimization are shown in Table 9.

Table 9. The ESTVs for the second round optimization

Position	ESTV	Shape	ESTV	Size	ESTV
Position#1	4.94E-03	hexagonal prism	4.94E-03	Large	4.94E-03
Position#2	3.45E-03	sphere	4.03E-03	Medium	5.42E-03
Position#3	2.23E-03	cylinder	4.75E-03	Small	6.28E-03
Position#4	1.04E-03				
η_P	**4.75**	η_{Sh}	**1.04**	η_{Si}	**1.27**

As shown in Table 9, the target's position can improve the ESTV the most, so the target's position should be optimized in the second round of optimization. Moreover, Position#1 has the highest ESTV, so the target's position is selected as Position #1. After the second round of optimization, the scheme becomes a large hexagonal prism target with Position #1 and Layout #5.

4.4 Third Round Sensitivity Analysis and Optimization

The third round of sensitivity analysis and optimization needs to consider two design parameters, i.e., the size and shape of the target. All new irradiation schemes are obtained based on the scheme after the second round of optimization. The ESTVs for the third round of optimization are shown in Table 10.

Table 10. The ESTVs for the third round optimization

Shape	ESTV	Size	ESTV
hexagonal prism	4.94E-03	Large	4.94E-03
sphere	4.03E-03	Medium	5.42E-03
cylinder	4.75E-03	Small	6.28E-03
η_{Sh}	**1.04**	η_{Si}	**1.27**

As shown in Table 10, the target's shape and size have similar effects on improving the ESTV, with the target's size slightly larger, so the target's size should be optimized in the third round optimization. Moreover, the small target has the

highest ESTV, so the small target is selected. After the third round of optimization, the scheme becomes a small hexagonal prism target with Position #1 and Layout #5.

4.5 Fourth Round Sensitivity Analysis and Optimization

The fourth round of sensitivity analysis and optimization needs to consider one design parameter, i.e., the shape of the target. All new irradiation schemes are obtained based on the scheme after the third round of optimization. The ESTVs for the fourth round of optimization are shown in Table 11.

Table 11. The ESTVs for the fourth round optimization

Shape	ESTV
hexagonal prism	6.28E-03
sphere	5.19E-03
cylinder	6.10E-03
η_{Sh}	**1.21**

As shown in Table 11, the hexagonal prism has the highest ESTV, so a hexagonal prism target is selected. After the fourth round of optimization, the scheme becomes a small hexagonal prism target with Position #1 and Layout #5.

4.6 Final Irradiation Scheme

The optimized scheme for producing Cf-252 is a small hexagonal prism target with Position #1 and Layout #5. Similarly, we optimized the schemes for producing Pu-238, Cm-242 and Cm-244. The final optimized irradiation schemes for producing Pu-238, Cm-242, Cm-244 and Cf-252 are given in Table 12. The comparison of production efficiency before and after optimization is shown in Figure 16.

Table 12. The final optimized irradiation schemes

Design parameters	**Pu-238**	**Cm-242**	**Cm-244**	**Cf-252**
Selection of moderator	zirconium hydride	zirconium hydride	zirconium hydride	zirconium hydride
Layout of moderator	Layout #6	Layout #6	Layout #6	Layout #5
Position of target	Position #1	Position #1	Position #1	Position #1

Shape of target	hexagonal	hexagonal	cylinder	hexagonal
Size of target	small	small	small	small

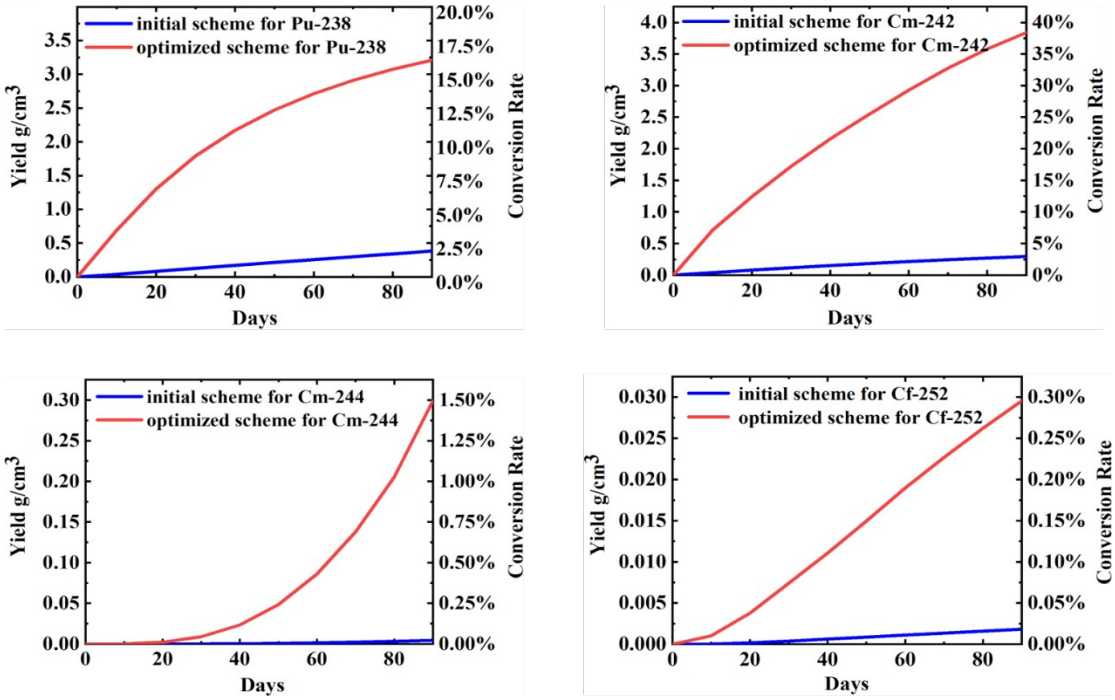

Figure 16. The comparison of the efficiency before and after optimization

After four rounds of sensitivity analysis and optimization, we can quickly obtain the optimal scheme for transplutonium isotopes production. As shown in Figure 16, the optimal scheme can effectively improve production efficiency compared with the initial scheme. The efficiency of Pu-238 is increased by 7.41 times, 11.98 times for Cm-242, 65.20 times for Cm-244 and 15.08 times for Cf-252. Therefore, the optimization strategy based on the rapid diagnosis method is helpful for transplutonium isotopes production.

5. CONCLUSION

The production of transplutonium isotopes with reactor irradiation is inefficient, and optimization studies are needed. The physics process of transplutonium isotopes production is complicated to analyze quantitatively. After grasping the physics nature and simplifying the complexity of the production process, we proposed the concept of "Single Energy Interval Value (SEIV)" and "Energy Spectrum Total Value (ESTV)" to realize the quantitative analysis of the production efficiency of transplutonium isotopes. A rapid diagnosis method for evaluating the radiation scheme based on the SEIV and ESTV is established. The optimization design for producing Cf-252, Cm-244, Cm-242 and Pu-238 is carried out based on the rapid diagnosis method. Compared with the initial scheme, the optimal scheme improves the efficiency of Pu-238 by 7.41 times, 11.98 times for Cm-242, 65.20 times for Cm-244 and 15.08 times for Cf-252.

This paper provides solutions to two key questions in the production of transplutonium isotopes: 1) how to find the optimal neutron spectrum for producing transplutonium isotopes, and 2) how to achieve the optimal neutron spectrum. For the first question, we use the SEIV and ESTV to achieve a detailed analysis of the

neutron spectrum around the target. For the second problem, we optimized the design parameters around the target to achieve the optimal neutron spectrum, effectively improving the computational efficiency.

The work in this paper realizes the refined analysis of transplutonium isotopes production and provides a theoretical basis for improving production efficiency. We will research energy spectrum conversion technology to achieve the optimal energy spectrum more finely in the future.

Acknowledgments

Author Contributions:
Qingquan Pan contributed to the concept, calculation, analysis, and writing;
Qingfei Zhao contributed to the concept, calculation, analysis;
Lianjie Wang, Bangyang Xia and Yun Cai contributed to review and funding;
Xiaojing Liu and Kan Wang contributed to review and code support.

Funding:
This work is sponsored by Natural Science Foundation of Shanghai [NO. 22ZR1431900] and Science and Technology on Reactor System Design Technology Laboratory.

Conflicts of Interest:
The authors declared that they have no conflicts of interest to this work. We declare that we do not have any commercial or associative interest represents a conflict of interest in connection with the work submitted.

Data Availability:
All data can be available through the Link:
https://pan.baidu.com/s/1MWjESVGZrP3fzMkctrtlIw
with the code “QPAN”

REFERENCE

[1] J. Bigelow, B. Corbett, L. King, et al. Production of transplutonium elements in the High Flux Isotope Reactor. ACS Symposium series 161, transplutonium elements-production and recovery. American Chemical Society, Washington, 1981, 3-18. https://doi.org/10.1021/bk-1981-0161.ch001

[2] J. Even, X. Chen, A. Soylu, et al. The NEXT project: Towards production and investigation of neutron-rich heavy nuclides. Atoms 2022, 10, 59. https://doi.org/10.3390/atoms10020059

[3] T. Dickel, A. Kankainen, A. Spataru, et al. Multi-nucleon transfer reactions at ion catcher facilities—A new way to produce and study heavy neutron-rich nuclei. Journal of Physics Conference Series, 2020, 1668, 012012. https://doi.org/10.1088/1742-6596/1668/1/012012

[4] G. Savard, M. Brodeur, J. Clark, et al. The N = 126 factory: A new facility to produce very heavy neutron-rich isotopes. Nuclear Instruments and Methods in Physics Research Section B: Beam Interactions with Materials and Atoms, 2020, 463, 258-261. https://doi.org/10.1016/j.nimb.2019.05.024

[5] Researchers urge action on medical-isotope shortage. Nature, 2009, 459, 1045. https://doi.org/10.1038/4591045b

[6] J. Tollefson. Reactor shutdown threatens world's medical-isotope supply. Nature, 2016. https://doi.org/10.1038/nature.2016.20577

[7] P. Gould. Medical isotope supplies dwindle. Nature, 2010. https://doi.org/10.1038/news.2010.70

[8] P. Gould, Medical isotope shortage reaches crisis level. Nature, 2009, 460, 312–313. https://doi.org/10.1038/460312a

[9] S. Hogle, C.W. Alexander, J.D. Burns, et al. Sensitivity studies and experimental evaluation for optimizing transcurium isotope production. Nuclear Science and Engineering, 2017, 185, 473-483. https://doi.org/10.1080/00295639.2016.1272973

[10] T. Tacev, B. Ptackova, V. Stmad. Cf-252 versus conventional gamma radiation in the brachytherapy of advanced cervical carcinoma. Strahlenther Onkol, 2003, 179, 379-384. https://doi.org/10.1007/s00066-003-1005-4

[11] M. Yu, S. Wang. The investigation and calculation of the transmutation paths for the production of Cf-252 in fast reactors. Annals of Nuclear Energy, 2020, 136,

107006. https://doi.org/10.1016/j.anucene.2019.107006
[12] R.C. Martin, J.B. Knauer, P.A. Balo. Production, distribution and application of Californium-252 neutron sources. Applied Radiation and Isotopes, 2000, 53, 785-792. https://doi.org/10.1016/S0969-8043(00)00214-1
[13] Z. Shen, X. Ouyang, H. Gao. Demand for aerospace materials and technology for China's deep space exploration. Aerospace Materials & Technology, 2021, 51(05).
https://doc.taixueshu.com/journal/20210079yhclgy.html
[14] S. Hogle. Optimization of transcurium isotope production in the High Flux Isotope Reactor. Doctoral dissertations at University of Tennessee, Knoxville, 2012.
https://trace.tennessee.edu/utk_graddiss/1529/
[15] S. Thompson, A. Chiorso, G. Seaborg. The new element californium (atomic number 98). Physical Review, 1950, 77, 838.
https://doi.org/10.1103/PhysRev.80.790
[16] P.R. Fields, M.H. Studier, H. Diamond, et al. Transplutonium elements in thermonuclear test debris. Physical Review, 1956, 102, 180.
https://doi.org/10.1103/PhysRev.102.180
[17] D. Schönenbach, F. Berg, M. Breckheimer, et al. Development, characterization, and first application of a resonant laser secondary neutral mass spectrometry setup for the research of plutonium in the context of long-term nuclear waste storage. Analytical and Bioanalytical Chemistry, 2021, 413, 3987–3997.
https://doi.org/10.1007/s00216-021-03350-3
[18] K. Dockx, E.C. Thomas, S. Thierry. ISOL Technique for the Production of 225 Ac at CERN-MEDICIS. Journal of Medical Imaging and Radiation Sciences, 2019, 50(4), 92. https://doi.org/10.1016/j.jmir.2019.11.077
[19] P. Schmor. Review of Cyclotrons for the Production of Radioactive Isotopes for Medical and Industrial Applications. Reviews of Accelerator Science and Technology, 2011, 4, 103-116. https://doi.org/10.1142/9789814383998_0005
[20] Y.S Lutostansky, V.I. Lyashuk. Production of Transuranium Nuclides in Pulsed Neutron Fluxes from Thermonuclear Explosions. JETP Letters, 2018, 107, 79-85.
https://doi.org/10.1134/S0021364018020108
[21] S. Hogle, G.I. Maldonado, C. Alexander. Increasing transcurium production efficiency through directed resonance shielding. Annals of Nuclear Energy, 2013, 60, 267-273. https://doi.org/10.1016/j.anucene.2013.05.018
[22] Y. Hou. Analysis of the world supply market for Californium-252 neutron source. China Nuclear Industry, 2015, 05, 24-26.
https://www.docin.com/p-1595472449.html
[23] S.M. Robinson, D.E. Benker, E.D. Collins, et al. Production of Cf-252 and other transplutonium isotopes at Oak Ridge National Laboratory. Radiochimica Acta, 2020, 108(9):737-746. https://doi.org/10.1515/ract-2020-0008
[24] D. Chandler, B.R. Betzler, E.E. Davidson, et al. Modeling and simulation of a High Flux Isotope Reactor representative core model for updated performance and safety basis assessments. Nuclear Engineering and Design, 2020, 366, 110752.
https://doi.org/10.1016/j.nucengdes.2020.110752
[25] C. Samantha, H. Riley. Campaign 78 - Production of 252Cf and the Recovery of Curium Feed Material at the Radiochemical Engineering Development Center,

2021, ORNL/TM-2020/1839. https://www.osti.gov/biblio/1782041
[26] G. Koehly, J. Bourges, c. Madic, et al. The production of transplutonium elements in France. ACS Symposium Series, 1981, 161, 19-40. https://doi.org/10.1021/bk-1981-0161.ch002
[27] Y.A. Karelin, Y.N. Gordeev, V.T. Filimonov, et al. Radionuclide production at the Russia State scientific center, RIAR. Applied Radiation and Isotopes, 1997, 48, 1585-1589. https://doi.org/10.1016/S0969-8043(97)00159-0
[28] J.B. Roberto, C.W. Alexander, R.A. Boll, et al. Actinide targets for the synthesis of super-heavy elements. Nuclear Physics A, 2015, 944, 99-116. https://doi.org/10.1016/j.nuclphysa.2015.06.009
[29] Y. Nagame, M. Hirata. Production and properties of tansuranium elements. Radiochimica Acta, 2011, 99, 377-393. https://doi.org/10.1524/ract.2011.1853
[30] M.B. Chadwick, M. Herman, P. Oblozinsky, et al. ENDF/B-VII.1 Nuclear Data for Science and Technology: Cross Sections, Covariances, Fission Product Yields and Decay Data. Nuclear Data Sheets, 2011, 112(12), 2887-2996. https://doi.org/10.1016/j.nds.2011.11.002
[31] M. Laatiaoui, S. Raeder. New developments in the production and research of actinide elements. Atoms, 2022, 10, 61. https://doi.org/10.3390/atoms10020061
[32] Q. Pan, H. Lu, D. Li, et al. A new nonlinear iterative method for SPN method. Annals of Nuclear Energy, 2017, 110, 920-927. https://doi.org/10.1016/j.anucene.2017.07.030
[33] Q. Pan, K. Wang. One-step Monte Carlo global homogenization based on RMC code. Nuclear Engineering and Technology, 2019, 51:1209-1217. https://doi.org/10.1016/j.net.2019.04.001
[34] Q. Pan, T. Zhang, X. Liu, et al. Optimal batch size growth for Wielandt method and Superhistory method. Nuclear Science and Engineering, 2021, 196(2), 183-192. https://doi.org/10.1080/00295639.2021.1968223
[35] F.B. Brown. Fundamentals of Monte Carlo particle transport. LA-UR-05-4983, Los Alamos National Laboratory, 2008. https://mcnp.lanl.gov/pdf_files/la-ur-05-4983.pdf
[36] Z. Xie. Physical analysis of nuclear reactor, Xi'an Jiaotong University Press, 2004.
[37] D. She, Y. Liu, K. Wang, et al. Development of burnup methods and capabilities in Monet Carlo code RMC. Annals of Nuclear Energy, 2013, 51, 289-294. https://doi.org/10.1016/j.anucene.2012.07.033
[38] D. She, K. Wang, G. Yu. Development of the point-depletion code DEPTH. Nuclear Engineering and Design, 2013, 258, 235-240. https://doi.org/10.1016/j.nucengdes.2013.01.007
[39] A. Nouri, P. Nagel, N. Soppera, et al. JANIS: A New Software for Nuclear Data Services. Journal of Nuclear Science and Technology, 2002, 39, 1480-1483. https://doi.org/10.1080/00223131.2002.10875385
[40] Q. Pan, N. An, T. Zhang, et al. Single-step Monte Carlo criticality algorithm. Computer Physics Communications, 2022, 279, 108439. https://doi.org/10.1016/j.cpc.2022.108439
[41] Q. Pan, T. Zhang, X. Liu, et al. SP3-Coupled Global Variance Reduction Method Based On RMC Code. Nuclear Science and Techniques, 2021, 32, 122. https://doi.org/10.1007/s41365-021-00973-0
[42] A. Ouardia, R. Alamia, A. Bensitela, et al. GEANT4 used for neutron beam

design of a neutron imaging facility at TRIGA reactor in Morocco. Nuclear Instruments and Methods in Physics Research Section A: Accelerator, Spectrometers, Detectors and Associated Equipment, 2011, 651, 21-27. https://doi.org/10.1016/j.nima.2011.02.096

[43] J. Mokhtari, F. Faghihi, J, Khorsandi. Design and optimization of the new LEU MNSR for neutron radiography using thermal column to upgrade thermal flux. Progress in Nuclear Energy, 2017, 100, 211-232. https://doi.org/10.1016/j.pnucene.2017.06.010

[44] K. Wang, Z. Li, D She, et al. RMC – A Monte Carlo code for reactor core analysis. Annals of Nuclear Energy, 82:121-129, 2015. https://doi.org/10.1016/j.anucene.2014.08.048

[45] N. Xoubi, R.T. Primm III. Modeling of the High Flux Isotope Reactor cycle 400. Oak Ridge National Laboratory. ORNL/TM-2004/251, 2004. https://citeseerx.ist.psu.edu/viewdoc/download?doi=10.1.1.605.281&rep=rep1&type=pdf

[46] S. Hogle, G.I. Maldonado. Modeling of the High Flux Isotope Reactor Cycle 400 with KENO-VI. Transactions of the American Nuclear Society, 104(1), 2011. https://www.ans.org/pubs/transactions/article-12169/